

## Electronic structure and equation of state of $\text{TiB}_2$

This article has been downloaded from IOPscience. Please scroll down to see the full text article.

1992 J. Phys.: Condens. Matter 4 8765

(<http://iopscience.iop.org/0953-8984/4/45/011>)

View [the table of contents for this issue](#), or go to the [journal homepage](#) for more

Download details:

IP Address: 171.66.16.96

The article was downloaded on 11/05/2010 at 00:49

Please note that [terms and conditions apply](#).

## Electronic structure and equation of state of $\text{TiB}_2$

De-Cheng Tian<sup>††</sup> and Xiao-Bing Wang<sup>†</sup>

<sup>†</sup> Department of Physics, Wuhan University, Wuhan 430072, People's Republic of China

<sup>††</sup> International Centre for Material Physics, Academia Sinica, Shenyang 110015, People's Republic of China

Received 28 April 1992, in final form 10 July 1992

**Abstract.** The electronic structure of  $\text{TiB}_2$  has been calculated using the self-consistent LMTO–ASA method. Our results have been compared with experimental and other theoretical work. We find that the pseudo-gap at the Fermi level is the competing effect of Ti 3d resonance and strong hybridization between Ti 3d and B 2p states. The bonding nature of  $\text{TiB}_2$  is discussed. We have carried out calculations of the equation of state (EOS) of  $\text{TiB}_2$ ; it is found that our first-principles calculated results support the universal model of EOS proposed by Vinet *et al.* The room-temperature isotherm is also plotted.

### 1. Introduction

Like many other borides,  $\text{AlB}_2$ -type transition-metal diborides possess some unique properties, such as a high melting point, hardness, chemical stability and metallic properties. They have attracted researchers in different fields. Many experimental and theoretical studies have been done on these materials (see, e.g., [1–4]). However, the bonding nature of these compounds is not very clear yet. Spear [5] studied the chemical bonding in  $\text{AlB}_2$ -type borides and concluded that the ability of metals to deform from a spherical shape appears to be very important in explaining why diborides are formed by a wide variety of metals. A tight-binding calculation of  $\text{TiB}_2$  was performed by Perkins and Sweeney [6] who found strong evidence of graphite band structure. On the basis of KKR calculations and the x-ray photoelectron spectrum, Ihara *et al* [7] proposed that the bonding nature of  $\text{ZrB}_2$  can be explained by a combination of the graphite bonding model of the boron network and the HCP metal bonding model of zirconium. From the viewpoint of orbital overlap, Burdett *et al* [8] studied the electronic structure of transition-metal borides with the  $\text{AlB}_2$  structure and found that the interaction of the orbitals of the transition metal with those of the planar graphite-like net of boron atoms and interaction with those of other metals are both important in influencing the properties of these species. These approaches are not consistent with each other. So further investigation of the electronic structure of transition-metal diborides is necessary. One purpose of this paper is to study the electronic structure and the bonding nature of  $\text{TiB}_2$  through the self-consistent band method of linear muffin-tin orbitals (LMTO) with the atomic sphere approximation (ASA). The result will be compared with experiments and other theoretical investigations.

## 2. Details of calculations

The LMTO-ASA [9] is used in our calculations. This method has been adopted by many researchers to study the electronic structure, ground-state properties and magnetic behaviour of different systems in recent years (see, e.g., [10-12]). Within this method, the volume of the unit cell is the sum of the total volume of the atomic spheres. Inside an atomic sphere, the effective one-electron potential is represented by two terms: the Coulomb and the exchange-correlation potentials. The Coulomb potential consists of the nuclear potential, the electron-electron repulsive potential (which may be obtained by solving the Poisson equation) and the Madelung potential (which represents the interaction between the electron and the charge centred at other atomic spheres). We used a computational procedure similar to that described in [13]. The calculations are self-consistent.

The crystal structure of  $\text{TiB}_2$  is  $\text{AB}_2$  type which is designated as C32. It is a simple-hexagonal lattice in which HCP Ti layers alternate with graphite-like B layers (figure 1). By choosing appropriate primitive lattice vectors, the atoms are positioned at  $\text{Ti}(0, 0, 0)$ ,  $\text{B}(\frac{1}{3}, \frac{2}{3}, \frac{1}{2})$  and  $\text{B}(\frac{2}{3}, \frac{1}{3}, \frac{1}{2})$  in the unit cell. This structure is quite close packed, and can be coped with efficiently and accurately by the LMTO-ASA method [9]. In table 1 are listed the crystallographic parameters [2] of  $\text{TiB}_2$  and the atomic configurations of Ti and B. Note that the Ti-Ti distance which is not given in table 1 is equal to  $a$ . Of particular interest is the fact that the Ti-B distance is approximately the sum of the atomic radii of Ti and B. The interaction between these two types of atom will be discussed in detail in the next section.

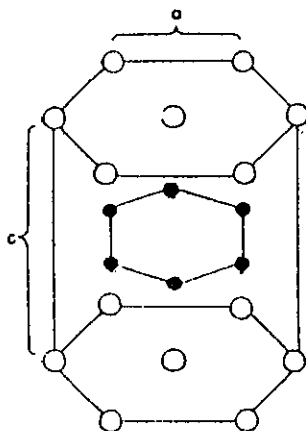


Figure 1. Crystal structure of  $\text{TiB}_2$ . The white spheres denote Ti atoms, and the black spheres B atoms.

Table 1. Crystallographic parameters and atomic configurations. TM-B and B-B denote the distances between neighbouring atoms.

Compound	$a$ (Å)	$c$ (Å)	TM-B (Å)	B-B (Å)	Atomic configuration
$\text{TiB}_2$	3.028	3.228	2.35	1.75	Ti $3d^24s^2$ ; B $2s^22p^1$

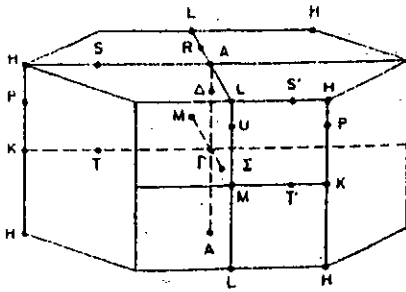


Figure 2. Brillouin zone of  $TiB_2$ .

The energy band is calculated on a uniform mesh of 64 points in the irreducible wedge of the Brillouin zone (figure 2). The radii of the Wigner-Seitz spheres are chosen according to the equality of the potential on different spheres. In the present calculation, they are 2.74 au and 2.18 au for Ti and B, respectively. Discussions on charge transfer in the next section are based on this selection. The convergence of eigenvalues is within 1 mRyd.

### 3. Electronic structure and bonding

Figure 3 shows the self-consistent band structure, and figure 4 the total and integrated densities of states (DOSS) of  $TiB_2$ . It is clear that  $TiB_2$  exhibits metallic behaviour. Three main peaks (A, B and C) exist in the total DOS curve (figure 4). Of these, peak A arises from the boron 2s states, the broad peak B corresponds to the boron 2p and titanium 3d states, and the sharp peak C above the Fermi level is related to the non-bonding titanium 3d states. The APW result for  $CrB_2$  [4] and the KKR result for  $ZrB_2$  [7] have the same general features. Table 2 lists a comparison of our results with experiments and previous calculations. In contrast with the width of the valence band, which shows excellent agreement with experiment, the DOS at the Fermi level (0.16 states  $eV^{-1}/cell$ ) shows a remarkable discrepancy with the experimental value (0.46 states  $eV^{-1}/cell$ ). This discrepancy (just as in [4]) appears to be caused by the lack of consideration of the electron-phonon interaction in our calculation.

Table 2. A comparison of our results with previous work.

	Width of valence band (eV)	DOS at the Fermi level (states $eV^{-1}/cell$ )
Data from [4] <sup>a</sup>	15.1	0.18
Data from [7] <sup>b</sup>	13.1, 11.0	0.22, 0.30
Experimental [7]	13.0	—
Experimental <sup>c</sup>	—	0.46
Our results	13.1	0.16

<sup>a</sup> Results from a rigid-band model of  $CrB_2$  calculated with the APW method.

<sup>b</sup> The KKR result for  $ZrB_2$ ; the two values correspond to KS exchange and Slater exchange, respectively.

<sup>c</sup> Computed from the electronic specific heat measured by Castaing *et al* [3].

From the band structure, one can find that only the fifth and sixth bands cross the Fermi level; there exists a pseudo-gap exactly at the Fermi level. Above the

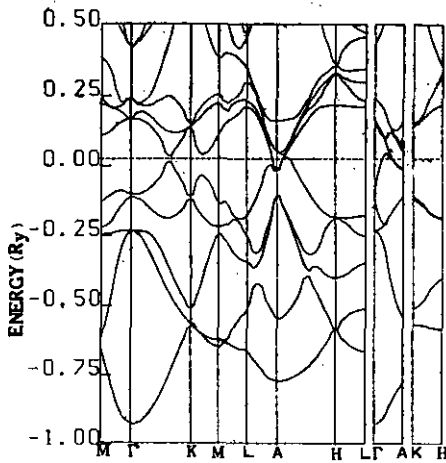


Figure 3. Band structure of  $\text{TiB}_2$ . The broken line represents the position of the Fermi level.

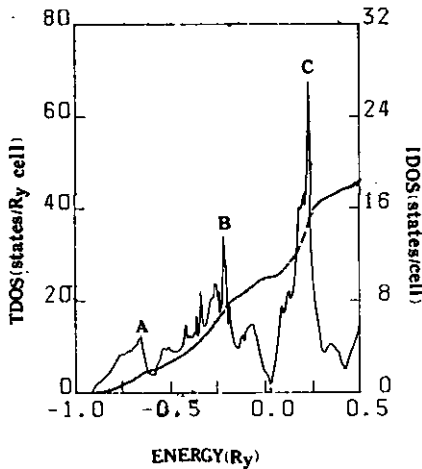


Figure 4. Total and integrated DOS of  $\text{TiB}_2$ ; the short line near the energy zero denotes the Fermi level.

pseudo-gap are the sharp non-bonding Ti 3d states, which divide the DOS into the bonding (below) and anti-bonding (above) states. Most of the states near the pseudo-gap are along the  $\Delta$  line of the Brillouin zone. The same minimum of  $\text{ZrB}_2$  was found by Ihara *et al* [7], but they did not give an explanation of this behaviour. It is interesting to note that the pseudo-gap exists not only in crystalline solids [14] and amorphous alloys [15], but also in quasi-crystals [12]. According to Pasturel *et al* [15], two mechanisms are responsible for the creation of the pseudo-gap. One of them (the hybridization origin) works reasonably well in the present case. The Ti 3d and B 2p partial DOS are plotted in figure 5. One can see that the hybridization is so large that, over the wide energy range from the bottom of valence band to 0.1 Ryd, the Ti 3d and B 2p states almost overlap completely. This hybridization not only gives important mixing between the Ti 3d and B 2p states but also lowers the energy of

the bonding states and raises the energy of anti-bonding states; so a pseudo-gap is produced and an enhancement in cohesive energy results. However, one may argue that the minimum near the Fermi level is simply the effect of sharp Ti d resonances which are characteristic of HCP transition metals (as Jepsen *et al* [16] have shown), and it has already been found in HCP titanium [17, 18]. We shall emphasize the fact that the minimum in the present case is much lower than the of HCP titanium ( $14.8 \text{ states Ryd}^{-1}/\text{atom}$  in the calculation of Vohra *et al* [17], and about  $10 \text{ states Ryd}^{-1}/\text{atom}$  according to Jepsen [18]). Only the d-d hybridization could not lead to this deep valley. So the pseudo-gap can be regarded as a competing effect of the d-d resonance and the strong hybridization between Ti 3d and B 2p states. The importance of the Ti-B interaction is also evident from the fact that  $\text{TiB}_2$  has a higher melting point and hardness than HCP titanium. To some extent, the importance of the metal-boron interaction had been recognized in transition-metal monoborides by Mohn and Pettifor [19] and in semi-borides by Mohn [20]. The fact that the Ti 3d and B 2p states are from different layers indicates that the strong interlayer bonding plays an important role in the formation of  $\text{TiB}_2$ . Therefore  $\text{TiB}_2$  cannot be called an exactly layered compound because there is no weak interaction in it.

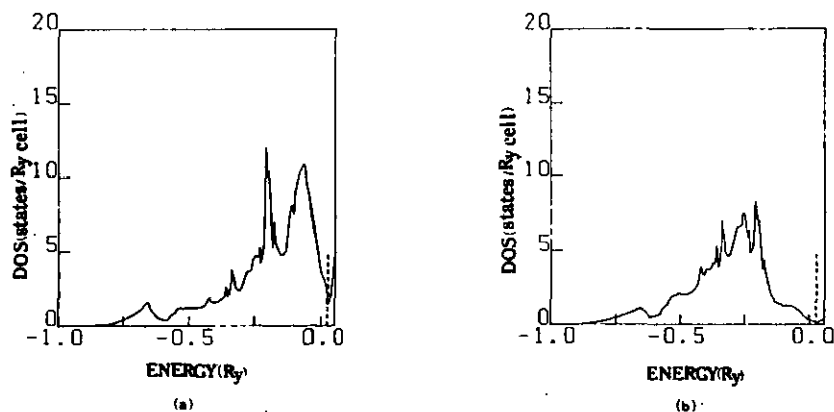


Figure 5. Ti 3d and half the B 2p partial DOSs of  $\text{TiB}_2$ : (a) Ti 3d, (b) B 2p. The broken line denotes the Fermi level.

Since large hybridization of Ti 3d and B 2p states exists, it is natural to consider the charge transfer as not so significant. This is consistent with the calculated result, which gives a charge transfer of about 0.25 electrons from Ti to B.

Ihara *et al* [7] had given a fine persuasive analysis of the band structure of  $\text{ZrB}_2$ , which was thought to be determined by the  $sp^2$  hybrid state and the  $p_z$  state of boron and the d and s state of zirconium. However, the hybridization between Zr 4d and B 2p states was not strongly emphasized. Like  $\text{ZrB}_2$ , our calculated DOS of  $\text{TiB}_2$  also has a shape composed of both the titanium DOS [17, 18] and the graphite DOS [21, 22] with disregard for the difference between the band widths. Considering the earlier discussions in this section, we assume that the Ti-B covalent bonding is as important as other bondings, if not more important in the electronic structure and therefore in influencing the physical properties of  $\text{TiB}_2$ .

#### 4. Equation of state

A universal relationship between the binding energies and distances between atoms has been discovered for bimetallic adhesion [23], chemisorption on metals [24] and metallic cohesion [25] (and then hypothesized for the equation of state (EOS) of nuclear matter [26]). Later Vinet *et al* [27] proposed a universal model of the equation of state (UEOS) for all classes of solids in compression. If we define  $x$  as  $(V/V_0)^{1/3}$ , and  $H(x)$  as  $x^2P(x)/3(1-x)$ , the  $\ln[H(x)]$  versus  $1-x$  curve should be nearly linear according to their theory:

$$\ln[H(x)] \simeq \ln B_0 + \eta(1-x) \quad (1)$$

and the EOS at a given temperature can be expressed as

$$P = [3B_0(1-x)/x^2] \exp[\eta(1-x)] \quad (2)$$

where  $B_0$  is the bulk modulus and  $\eta$  a constant at given temperatures.

Although different classes of solids exhibit different bonding natures, Vinet *et al* [27] have argued that in compression the form of the pressure-volume relation is dominated by the overlap interaction for all classes of solids, and empirical evidence of applicability of the UEOS for hydrogen and deuterium, alkali and other metals, ionic crystals, rare-gas solids, some polymers and a glass has been demonstrated [28]. These solids have all kinds of bond (metallic, covalent, ionic and van der Waals), although they are mostly dominated by one type of bond. In the case of  $\text{TiB}_2$ , the bonding nature can be regarded as a combination of metallic and covalent bonding (also partly ionic bonding because of the existence of charge transfer) as discussed in the previous section. So is the UEOS suitable to describe  $\text{TiB}_2$  of mixed bonding?

In order to test the applicability of the UEOS to  $\text{TiB}_2$ , self-consistent calculations have been performed for several different volumes. In all these calculations, the  $c/a$  ratio is kept constant at 1.066. Near the equilibrium volume ( $p \simeq 0$ ), a linear approximation between pressure and volume (harmonic approximation) is made to evaluate the value of  $V_0$ . It is found that the lattice parameter in this approximation is 2.895 Å, which differs by 4.4% from the experimental value.  $B_0$  is also obtained as 3.77 Mbar. Using equation (2), we find  $\eta$  to be 6.28. Then we have computed the values of  $\ln[H(x)]$  and  $1-x$  and made the least-mean-squares linear fit to see whether a linear relationship exists. The result shows surprisingly good agreement with the UEOS; with a correlation coefficient of 0.99, there is excellent linearity. The calculated bulk modulus  $B_0$  is given as 3.7 Mbar and  $\eta$  as 6.31. One can see self-consistency of our results within the theory of Vinet *et al*. The value of the bulk modulus is consistent with experiment if we take the Poisson ratio as about 0.25 (the elastic constant given in [1] is 5.6 Mbar). The calculated  $\ln[H(x)]$  versus  $1-x$  curve is plotted in figure 6, as well as the best-fit line.

To obtain the room-temperature isotherm, we use the well known Grüneisen equation in the Debye approximation  $P_T = \gamma C_V T/V$  [29] to evaluate the thermal contribution to the pressure. Here  $C_V$  is the room-temperature specific heat and  $\gamma$  the Grüneisen parameter, which is taken as  $\gamma = V\alpha B/C_V$ , where  $\alpha$  is the thermal expansion coefficient and  $B$  the bulk modulus. So we have

$$P_T = \alpha BT \quad (3)$$

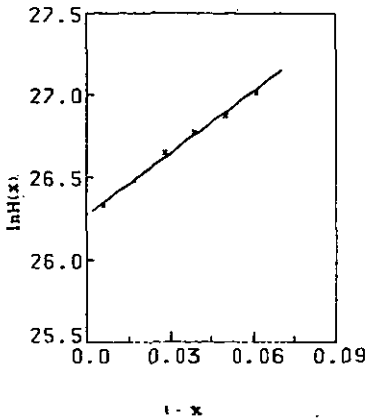


Figure 6. The calculated  $\ln[H(x)]$  versus  $1-x$  curve for  $\text{TiB}_2$ :  $x$ , calculated result; —, best-fit line.

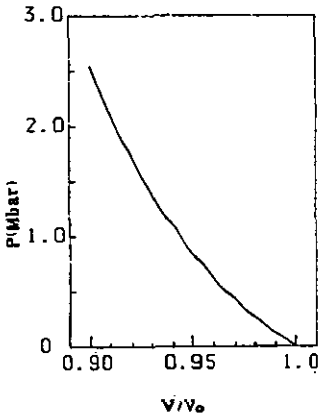


Figure 7. Calculated room-temperature isotherm of  $\text{TiB}_2$ .

for the room-temperature thermal pressure. The value of  $\alpha$  is taken from [1]. In this approach, the zero-temperature pressure comes from equation (2) using the calculated  $V_0$ ,  $B_0$  and  $\eta$ , while the thermal pressure is determined by employing the Grüneisen equation in the Debye approximation using an experimental value  $\alpha$ . Figure 7 illustrates our calculated room-temperature isotherm. To our regret, we have no experimental data to compare with our theoretical calculation, which must be taken as a guide to future experiments.

## 5. Conclusion

In conclusion, our band calculations using the LMTO-ASA method give an accurate description of the electronic structure of  $\text{TiB}_2$ . The pseudo-gap in  $\text{TiB}_2$  is the result of the competing effects of Ti d resonance and the strong Ti 3d and B 2p hybridization. The Ti-B covalent bonding is as important as other bondings, if not more important,



in the electronic structure and therefore in influencing the physical properties of  $\text{TiB}_2$ . Our first-principles calculations of the EOS support the UEOS of Vinet *et al.* The room-temperature isotherm of  $\text{TiB}_2$  is also given.

### Acknowledgments

Thanks are due to the National Science Foundation of China for financial support and to the National Laboratory of New Technology of Composite Materials for its partial support.

### References

- [1] Matkovich V I (ed) 1977 *Boron and Refractory Borides* (Berlin: Springer)
- [2] Samsonov G V, Serebriakova T T and Neronov Y A 1975 *Borides* (Moscow: Atomizdat) (in Russian)
- [3] Castaing J, Costa P, Heritier M and Lederer P 1972 *J. Phys. Chem. Solids* **33** 533  
Castaing J, Danan J and Rieux M 1972 *Solid State Commun.* **10** 563  
Castaing J, Caudron R, Toupance G and Costa P 1969 *Solid State Commun.* **7** 1453
- [4] Liu S H, Kopp L, England W B and Myron H W 1975 *Phys. Rev. B* **11** 3463
- [5] Spear K E 1976 *J. Less-Common Met.* **47** 195
- [6] Perkins P G and Sweeney A V J 1976 *J. Less-Common Met.* **47** 165
- [7] Ihara H, Hirabayashi M and Nakagawa H 1977 *Phys. Rev. B* **16** 726
- [8] Burdett J K, Canadell E and Miller G J 1986 *J. Am. Chem. Soc.* **108** 6561
- [9] Andersen O K 1975 *Phys. Rev. B* **12** 3060
- [10] Jaswal S S 1990 *Phys. Rev. B* **41** 9697
- [11] Guo G Y and Liang W Y 1987 *J. Phys. C: Solid State Phys.* **20** 4315
- [12] Fujiwara T and Yokokawa T 1991 *Phys. Rev. Lett.* **66** 333
- [13] Skriver H L 1984 *The LMTO Method* (Berlin: Springer)
- [14] Xu J and Freeman A J 1989 *Phys. Rev. B* **40** 11927
- [15] Pasturel A, Colinet C and Hicter P 1985 *Physica B* **132** 177
- [16] Jepsen O, Andersen O K and Mackintosh A R 1975 *Phys. Rev. B* **12** 3084
- [17] Vohra Y K, Sikka S K and Chidambaram R 1979 *J. Phys. F: Met. Phys.* **9** 1771
- [18] Jepsen O 1975 *Phys. Rev. B* **12** 2998
- [19] Mohn P and Pettifor D G 1988 *J. Phys. C: Solid State Phys.* **21** 2829
- [20] Mohn P 1988 *J. Phys. C: Solid State Phys.* **21** 2841
- [21] Willis R F, Fritton B and Painter G S 1974 *Phys. Rev. B* **9** 1926
- [22] MacFeely F R, Kowalozyk S P, Ley L, Gawaell R G, Pollak R A and Shirley D A 1974 *Phys. Rev. B* **9** 5288
- [23] Rose J H, Ferrante J and Smith J R 1981 *Phys. Rev. Lett.* **47** 675  
Ferrante J and Smith J R 1985 *Phys. Rev. B* **31** 3427  
Smith J R and Ferrante J 1985 *Mater. Sci. Forum* **4** 21
- [24] Smith J R, Ferrante J and Rose J H 1982 *Phys. Rev. B* **25** 1419
- [25] Ferrante J, Smith J R and Rose J H 1983 *Phys. Rev. Lett.* **50** 1385; 1983 *Phys. Rev. B* **28** 1835
- [26] Rose J H, Vary J P and Smith J R 1984 *Phys. Rev. Lett.* **53** 344
- [27] Vinet P, Ferrante J, Smith J R and Rose J H 1986 *J. Phys. C: Solid State Phys.* **19** L467
- [28] Vinet P, Rose J H, Ferrante J and Smith J R 1989 *J. Phys.: Condens. Matter* **1** 1941
- [29] McMahan A K, Skriver H L and Johansson B 1981 *Physics of Solids Under High Pressures* ed J S Schilling and R N Shelton (Amsterdam: North-Holland) p 169